Spin noise spectroscopy of quantum dot molecules

Dibyendu Roy, Yan Li, Alex Greilich, Yuriy V. Pershin, Avadh Saxena, and Nikolai A. Sinitsyn

Phys. Rev. B **88**, 045320 — Published 26 July 2013

DOI: 10.1103/PhysRevB.88.045320

Spin noise spectroscopy of quantum dot molecules

Dibyendu Roy[1,2], Yan Li[3], Alex Greilich[4], Yuriy V. Pershin[5], Avadh Saxena[1], Nikolai A. Sinitsyn[1]
[1] *Theoretical Division, Los Alamos National Laboratory, Los Alamos, New Mexico 87545, USA*
[2] *Center for Nonlinear Studies, Los Alamos National Laboratory, Los Alamos, New Mexico 87545, USA*
[3] *National High Magnetic Field Lab, Los Alamos National Laboratory, Los Alamos, New Mexico 87545, USA*
[4] *Experimentelle Physik 2, Technische Universität Dortmund, D-44221 Dortmund, Germany and*
[5] *Department of Physics and Astronomy and USC Nanocenter, University of South Carolina, Columbia, SC 29208, USA*

We discuss advantages and limitations of the spin noise spectroscopy for characterization of interacting quantum dot systems on specific examples of individual singly and doubly charged quantum dot molecules (QDMs). It is shown that all the relevant parameters of the QDMs including tunneling amplitudes with spin-conserving and spin-non-conserving interactions, decoherence rates, Coulomb repulsions, anisotropic g-factors and the distance between the dots can be determined by measuring properties of the spin noise power spectrum.

PACS numbers: 72.70.+m, 72.25.Rb, 78.67.Hc

I. INTRODUCTION

Spins of electrons or holes in two interacting neighboring quantum dots (QDs) represent a building block for realization of a scalable solid-state quantum information platform[1]. Such a block unit, called a quantum dot molecule (QDM), can be e.g. electrostatically defined[2] or it can be formed from two closely spaced self-assembled InAs/GaAs QDs, in which relative energy levels and charging of the two dots can be tuned by an applied electric field when the QDM is embedded in the Schottky diode structure[3–5]. By time-dependent manipulations with external fields and by varying coupling parameters quantum gate operations should be realizable. Precise control over the structure parameters is required for spin initialization, readout, and coherent manipulation for a practical application in quantum information processing. However, the number of parameters describing the QDM in a diode structure is relatively large[1,6]. These include, the relative energies of singly and doubly occupied quantum dots, tunneling amplitudes, effects of spin flips due to spin-orbit coupling and difference of g-factors[7]. Optical studies[3,4] have been used to investigate selective tunneling of electrons or holes[5,8], origins of spin fine structure[9] and conditional quantum dynamics[10].

In this work, we explore the potential of an alternative approach, called the spin noise spectroscopy (SNS) that has already been demonstrated as a powerful probe of physics of hole or electron spins localized in separated QDs[11,12]. In this approach, the spin noise power spectrum is obtained by measuring the fluctuations of the optical Faraday rotation of a linearly polarized beam passing through a region with spins. Although up to now, the main focus of experiments was on the spin noise of an aggregate ensemble of hundreds of QDs; there is no fundamental limit on SNS to achieve the level of a single spin sensitivity using Faraday rotation fluctuations. For example, the Faraday rotation signal of a single spin has already been demonstrated experimentally[13]. Recently, an experiment showed the possibility to measure spin noise from a single InGaAs QD by means of resonant fluorescence[14].

Anticipating the future progress with increasing sensitivity of SNS to resolving single spin fluctuations, in this work, we explore the potential of this approach for characterization of solid state nanostructures on a specific example of QDMs. We will show that SNS may provide several advantages: First, characterization of a QDM can be achieved at the thermodynamic equilibrium, without applying a strong perturbation; Second, details of the spin noise power spectrum can be obtained with high resolution, which can be used not only to determine resonant frequencies, but also to find the relative integrated noise power of different noise power peaks, as it was demonstrated in atomic gases[15].

Moreover, spin noise is derived from the measured Faraday rotation signal of a light beam. The latter may couple to spins of different dots with different strengths due to the difference in the frequency detuning between the measurement beam and the optical resonant frequencies of two dots. For example, if the measurement is sensitive only to the spin of one of the QDs, then the tunneling of an electron or hole will be observed as a change in the measured signal even if physically the spin does not flip. We will argue that this effect provides additional means for the detection of tunneling in the QDM even in the absence of external magnetic fields.

The structure of this article is as follows. In Sec. II we provide basic information about the state of the art of SNS and the definition of the spin noise power. In Sec. III we consider the model of a QDM charged by a single electron or hole and propose steps for its full characterization. In Sec. IV we investigate possible characteristics of a more complex case of a QDM with two holes or electrons. We summarize our results in Sec. V.

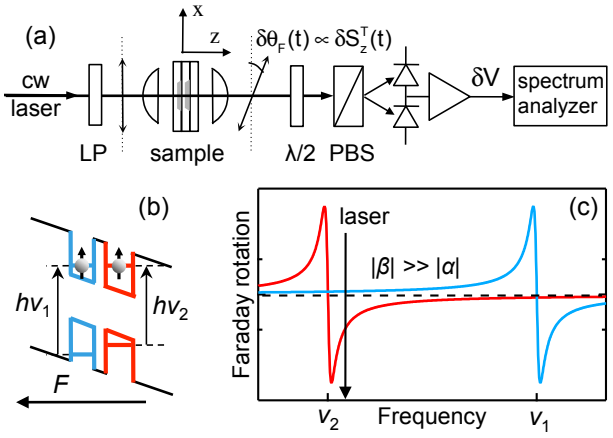

FIG. 1. (a) Potential experimental setup. LP: linear polarizer; $\lambda/2$: half-wave plate; PBS: polarizing beam splitter. (b) Schematic band structure of a QDM with two charged electrons in an applied electric field F. (c) Faraday rotation as a function of laser frequency. Due to asymmetries in size, strain and shape, the two QDs have different transition energies. The laser linewidth is much narrower than the absorption linewidth, and close to one QD transition energy (i.e. close to the right quantum dot), so the coupling coefficient $|\beta| \gg |\alpha|$.

II. SPIN NOISE POWER SPECTRUM

Spin noise spectroscopy was introduced by Aleksandrov and Zapasskii[16] who employed off-resonant optical Faraday rotation to passively detect ground-state spin fluctuations in a gas of sodium atoms. Later it has been refined and applied to measure various dynamical properties of electron (and hole) spins in alkali vapors[15], bulk GaAs[17,18], quantum wells[19] and self-assembled QDs[11]. Dynamic spin fluctuations generate spontaneous spin precession and decay with the same characteristic energy and timescales as the macroscopic magnetization of initially polarized spins. Hence, the physical parameters, such as g-factors, hyperfine coupling, and spin coherence lifetimes can be determined by measuring only the correlation spectra[20,21].

We show in Fig. 1(a) a potential schematic of the optical magnetometer to "listen" to spin noise of a single or double electrons/holes in a QDM. A linearly polarized continuous wave (CW) laser beam is tuned to have frequency near the resonance of transition from the ground-state of the QDM to the higher energy level of one of the QDs. Random fluctuations of the electron spins along the incident beam (z-direction), $\delta S_{Lz}(t)$ and $\delta S_{Rz}(t)$ impart Faraday rotation fluctuations $\delta\theta_F(t)$ on the transmitted probe-laser beam via spin-dependent refraction indices for right- and left-circularly polarized light $n^{\pm}(\nu)$ where ν is the frequency of the incident beam[18,22]. Using a half-wave plate and a balanced photodiode, these Faraday rotation fluctuations are detected and converted to fluctuating voltage signals which are amplified and measured by fast digitizers. Power spectra of the time-domain voltage signals are computed with fast-Fourier transform algorithms. The Faraday rotation $\theta_F(\nu)$ scales linearly with $(n^+(\nu) - n^-(\nu))$, namely, the difference between spin-up and spin down electron densities in the absence of a magnetic field along the direction of laser beam propagation.

The incident laser beam is detuned sufficiently from the optical transition energy of both dots to ensure no absorption of the beam energy by the QDs and the interaction of photons with a QD is mostly sensitive to the dispersive part of the QD dielectric function. Importantly, due to asymmetries in the structures of the self-assembled QDs (variations in size, strain, and shape in different QDs), the transition energy from a single resident electron (hole) to negatively (positively) charged trion state can differ from QD to QD [Fig. 1(b)]. The spin noise power spectrum from the QDM is then given by the light intensity correlation function[22],

$$S_N(\omega) = \int_0^\infty dt \ \cos(\omega t)\langle S_z^T(t) S_z^T(0)\rangle, \qquad (1)$$

where we introduced the *weighted spin*: $S_z^T(t) = \alpha S_{Lz}(t) + \beta S_{Rz}(t)$. Here α and β determine the coupling strengths of the incident laser beam with the spin in the left and right QDs, and $\langle O\rangle$ denotes thermal average of the operator O. In the framework of the weak measurement theory, α and β are proportional to the small probabilities per unit of time to collapse the wave function of the QDM and thus obtain the value of, respectively, S_{Lz} or S_{Rz} at this moment. The difference $\alpha \neq \beta$ is due to the fact that the detuned laser beam may have closer frequency to the resonant frequency of one QD compared to the other because the detuning in the laser frequency is much smaller compared to the frequency difference between the resonances of the two dots [Fig. 1(c)]. Therefore the coupling of the incident laser beam with the two QDs is expected to be different, i.e., $\alpha \neq \beta$[23]. In fact, the difference in the detuning energies of two dots is typically as large as a few meVs, while the Faraday rotation is inversely proportional to the detuning, which means that generally one should find the regime of either $\alpha \gg \beta$ or $\alpha \ll \beta$. For completeness, we will consider an arbitrary ratio α/β in the following calculations with easily obtainable limiting cases.

In order to predict the spin noise power using Eq. (1), we calculate eigenvalues and eigenfunctions of the Hamiltonian of the system, and use them to evaluate the thermal average of the spin-spin correlation. Let us call λ_i and $|\lambda_i\rangle$ eigenvalues and eigenfunctions of the Hamiltonian, respectively. Now we write the thermal average of the spin correlation function as,

$$\langle S_z^T(t)S_z^T(0)\rangle = \sum_{i,j} \frac{e^{-\lambda_i/k_BT-|t|/\tau_{ij}}}{\mathcal{Z}} e^{i(\lambda_j-\lambda_i)t} |\langle\lambda_i|S_z^T(0)|\lambda_j\rangle|^2, \quad (2)$$

where for each resonance with energy difference $\lambda_j - \lambda_i$, we introduced a phenomenological dephasing time τ_{ij}. Here the partition function $\mathcal{Z} = \sum_i e^{-\lambda_i/k_BT}$, k_B is the Boltzmann constant, and T is temperature. In the following formulas, in order to simplify notation, we will often suppress decoherence parameters τ_{ij} in the expression for spin correlators, assuming that they are always there. At temperatures $\sim$ 5K the Boltzmann factor can be disregarded if the tunneling amplitude is below 1 GHz (i.e., ~ 1 μeV). We will assume such cases of weakly coupled QDs.

One can easily suppress tunneling of electrons by applying an electric field F that creates an extra energy difference 2ϵ between an electron occupying the left or the right dot, $2\epsilon = edF$, where d is the distance between the dots. Relative strengths of parameters α and β can be determined simultaneously along with Lande g-factors by suppressing tunneling and then applying a magnetic field $\mathbf{B}$ of 100-1000 Gauss magnitude. For example, the effective Hamiltonian of a doubly charged QDM in a magnetic field $\mathbf{B} \equiv \{b_x, b_y, b_z\}$ can be written as $H_Z = \mu_B \mathbf{B}\cdot(\mathbf{g}_L^e\cdot\mathbf{S}_L + \mathbf{g}_R^e\cdot\mathbf{S}_R)$. We use $\mathbf{g}_L^e \in \{g_{L\|}^e, g_{L\perp}^e\}$ and $\mathbf{g}_R^e \in \{g_{R\|}^e, g_{R\perp}^e\}$ where $g_{L\|}^e$ and $g_{L\perp}^e$ ($g_{R\|}^e$ and $g_{R\perp}^e$) are the g-factors of electron in the left (right) QD along the direction (z direction) of the incident linearly polarized laser beam, and the plane perpendicular to z direction respectively, μ_B is the Bohr magneton. The spin of a single electron or hole inside a QDM makes Larmor precession with a frequency that depends on its position in the QDM. The spin noise correlator in a field b_x at temperatures $\sim 5K$ is given by

$$\langle S_z^T(t)S_z^T(0)\rangle = \frac{1}{2}\big(\alpha^2 e^{-t/T_{2L}}\cos(\mu_B g_{L\perp}^e b_x t) + \beta^2 e^{-t/T_{2R}}\cos(\mu_B g_{R\perp}^e b_x t)\big), \quad (3)$$

where we take into account phenomenological spin decoherence times T_{2L} and T_{2R} for the left and right quantum dots. When dots are decoupled, such decoherence rates can be as small as 1MHz[24]. The spin noise power spectrum then becomes the sum of two relatively sharp Lorentzian peaks.

$$S_N(\omega) = \frac{1}{4}\Big(\frac{\alpha^2/T_{2L}}{(\omega-\mu_B g_{L\perp}^e b_x)^2 + 1/T_{2L}^2} + \frac{\beta^2/T_{2R}}{(\omega-\mu_B g_{R\perp}^e b_x)^2 + 1/T_{2R}^2}\Big). \quad (4)$$

Two finite frequency peaks in the noise power spectrum are centered around $\mu_B g_{L\perp}^e b_x$ and $\mu_B g_{R\perp}^e b_x$. Thus, the in-plane g-factors of electron in both the QDs can be determined directly from positions of these peaks. Similarly one can measure $g_{L\|}^e$ and $g_{R\|}^e$ by applying an additional out-of-plane field b_z and measuring the shift of the Larmor frequencies or changes in the relative areas of power peaks[12].

Importantly, as peaks are well separated, one can separately measure their areas by integrating spin noise power over the regions around individual peaks. Such an individual peak integrated noise power does not depend on relaxation rate. For example, the ratio of the areas of the two peaks in Eq. (4) would be $(\alpha/\beta)^2$, which provides the estimate of the coupling of the incident laser beam with the electron in either QD.

We study two cases: (1) A QDM is charged with only a single electron that can hop between two dots, and (2) both dots are charged with an electron. The Hamiltonians for QDMs containing one excess hole or two excess holes are qualitatively similar to those of excess electrons.

III. SPIN NOISE FROM SINGLE ELECTRON CHARGED QDM

We consider only the lowest confined energy levels for electrons of each QD of a QDM. Even if both dots are grown under nominally identical conditions, the strain and the asymmetry generally lead to non-degenerate dots with slightly different energy levels. The applied electric field (F) controls the relative energy levels of the two dots at a distance d between the two dots. It can be used to tune either electron or hole energy levels into the resonance. Electrons and holes can then tunnel through the barrier separating the two dots[25]. The spatial basis states for the electrons localized in the left and right QD are given by the two lowest orthogonal states $\phi_L(\mathbf{r})$ and $\phi_R(\mathbf{r})$. Similarly we define spin basis states $|\sigma, 0\rangle$ and $|0, \sigma\rangle$ for an electron with spin σ localized in the left and right QD, respectively.

When the QDM is charged with a single electron the full wave-function of QDM is given by $\phi_L(\mathbf{r})|\sigma, 0\rangle$ or $\phi_R(\mathbf{r})|0, \sigma\rangle$ depending on the position of the electron in the QDM. Electron or hole tunneling between two quantum dots can be both spin independent and with a spin flipping with amplitudes γ_c and γ_{nc}, respectively. The latter is possible due to the spin-orbit coupling. We fix the basis so that the spin-conserving tunneling γ_c is real, and then we assume that γ_{nc} is generally complex. In addition to the spin-orbit interaction (which we have incorporated in γ_{nc}) there are two other sources of spin-dependent local interaction, one is the Zeeman coupling due to an external magnetic field and the other is the hyperfine coupling between electron spins and nuclear spins in a QD. The latter field is time-dependent and usually is considered the major source of decoherence at low (below 5-10 K) temperatures[12]. In order to ob-

serve coherent tunneling, this field should be weak so that its other effects could be disregarded. For example, the Overhauser field for hole doped InAs QDs is about 25 Gauss[12,26]. Alternatively, the decoherence time of 37 ns in electrostatically defined GaAs quantum dots[2] would also be sufficient for studies of coherent spin interactions by SNS. Henceforth, we will assume the case of such QDMs in which the Overhauser field amplitude is negligible in comparison to other parameters, such as the tunneling amplitude, and assume that its effect is reduced to introducing the finite decoherence rate at time scales of 10-100 ns.

The most general Hamiltonian $H^{(1)}$ of the QDM charged with one electron, which is allowed by the time-reversal symmetry at zero magnetic field, in the basis $\{|\uparrow,0\rangle, |\downarrow,0\rangle, |0,\uparrow\rangle, |0,\downarrow\rangle\}$ reads

$$H^{(1)} = \begin{pmatrix} \epsilon + g_{L\parallel} b_z & g_{L\perp} b_- & \gamma_c & \gamma_{nc} \\ g_{L\perp} b_+ & \epsilon - g_{L\parallel} b_z & -\gamma_{nc}^* & \gamma_c \\ \gamma_c & -\gamma_{nc} & -\epsilon + g_{R\parallel} b_z & g_{R\perp} b_- \\ \gamma_{nc}^* & \gamma_c & g_{R\perp} b_+ & -\epsilon - g_{R\parallel} b_z \end{pmatrix}, \tag{5}$$

where ϵ is the bias between the two QDs, which can be controlled by an external electric field; $g_{L\parallel} = \mu_B g^e_{L\parallel}/2$, $g_{R\parallel} = \mu_B g^e_{R\parallel}/2$, $g_{L\perp} = \mu_B g^e_{L\perp}/2$, $g_{R\perp} = \mu_B g^e_{R\perp}/2$ and $b_\pm = b_x \pm i b_y$. In (5), the signs of tunneling terms are chosen to ensure the time reversal symmetry of the spin-orbit coupling.

In the absence of a magnetic field, the eigenvalues of the Hamiltonian in Eq. (5) are doubly degenerate. The eigenvalues are $\lambda_1 = -\lambda \equiv -\sqrt{\gamma_c^2 + |\gamma_{nc}|^2 + \epsilon^2}$, $\lambda_2 = -\lambda$, $\lambda_3 = \lambda$, $\lambda_4 = \lambda$, and the corresponding orthonormal eigenvectors $|\lambda_i\rangle$ $(i = 1, 2, 3, 4)$ can be derived explicitly. We find from Eq. (2) using λ_i and $|\lambda_i\rangle$ after disregarding the Boltzmann factor $e^{-\lambda_i/k_BT}$ and suppressing the decoherence parameters τ_{ij},

$$\langle S_z^T(t) S_z^T(0)\rangle = \frac{(\alpha^2+\beta^2)(\epsilon^2+\lambda^2) + 2\alpha\beta(\gamma_c^2 - |\gamma_{nc}|^2)}{16\lambda^2} + \frac{(\alpha^2+\beta^2)(\gamma_c^2+|\gamma_{nc}|^2) - 2\alpha\beta(\gamma_c^2-|\gamma_{nc}|^2)}{16\lambda^2}\cos(2\lambda t). \tag{6}$$

The spin noise power spectrum, at positive frequencies, would correspond to one peak that is centered at a frequency 2λ, and one zero-frequency peak. Hence, one can determine the eigenvalues of the Hamiltonian experimentally from the position of the finite-frequency peak. In addition, if we probe the spin noise from the individual QDs of the QDM, we can calculate both the single-particle energy of the QDs and the total magnitude of tunneling easily without tuning the electric field, for example, when $\alpha = 0$ and $\beta = 1$ (which is a likely case) the spin noise correlator is given by

$$\langle S_{Rz}(t) S_{Rz}(0)\rangle = \frac{(\epsilon^2+\lambda^2)}{16\lambda^2} + \frac{(\gamma_c^2+|\gamma_{nc}|^2)}{16\lambda^2}\cos(2\lambda t). \tag{7}$$

Hence, by measuring the relative integrated powers of separate peaks, one can determine the bias ϵ separately from the effective tunneling parameter $\sqrt{\gamma_c^2+|\gamma_{nc}^2|}$. In the limit $\epsilon \gg \gamma_c, |\gamma_{nc}|$, the finite frequency peak in Eq. (7) vanishes, and $\langle S_{Rz}(t) S_{Rz}(0)\rangle \to 1/8$. The meaning of the latter result is the following: When tunneling is suppressed, the zero-frequency peak becomes merely the average of the square of the spin operator $(S_{Rz})^2 = 1/4$. Since all states are equally probable, an electron will spend half of the time on average in the unobservable QD, which reduces the noise power by an additional factor of 1/2.

For self-assembled QDs it is easy to tune the single-particle energy of the QDs in the QDMs by an applied electric field. In fact, the applied electric field is also required to charge the QDs with a single electron in the reverse bias of the Schottky diode configuration. Therefore we can bring the QDs in a symmetric energy configuration, in which ϵ vanishes. In the case of comparable α and β, it is possible to derive the values of γ_c and $|\gamma_{nc}|$ from the relative area (the ratio of the areas) of the zero and finite frequency peaks, which is $[(\alpha^2+\beta^2)(\gamma_c^2+|\gamma_{nc}|^2) + 2\alpha\beta(\gamma_c^2-|\gamma_{nc}|^2)]/[(\alpha^2+\beta^2)(\gamma_c^2+|\gamma_{nc}|^2) - 2\alpha\beta(\gamma_c^2-|\gamma_{nc}|^2)]$ with known values of α, β. We remind here that the ratio α/β can be found by measuring spin noise at a strong bias in an external magnetic field.

Alternatively, one can recover all parameters of the Hamiltonian by applying a weak (in comparison to the tunneling rate) in-plane magnetic field. To assess the effect of a weak magnetic field we perform a perturbative calculation. The degenerate perturbation theory predicts that the lowest order effect of the magnetic field is a splitting of the otherwise degenerate eigenenergies:

$$\tilde\lambda_{1x\pm} = -\lambda \pm \frac{b_x}{2}\Big\{(g_{L\perp}+g_{R\perp})^2 + \frac{2\epsilon(-g_{L\perp}^2+g_{R\perp}^2)}{\lambda} + \frac{\epsilon^2(g_{L\perp}-g_{R\perp})^2 - 4g_{L\perp}g_{R\perp}\mathrm{Re}[\gamma_{nc}]^2}{\lambda^2}\Big\}^{1/2},$$

$$\tilde\lambda_{2x\pm} = +\lambda \pm \frac{b_x}{2}\Big\{(g_{L\perp}+g_{R\perp})^2 + \frac{2\epsilon(g_{L\perp}^2-g_{R\perp}^2)}{\lambda} + \frac{\epsilon^2(g_{L\perp}-g_{R\perp})^2 - 4g_{L\perp}g_{R\perp}\mathrm{Re}[\gamma_{nc}]^2}{\lambda^2}\Big\}^{1/2}.$$

Thus, there are two low frequency peaks centered around $(\tilde\lambda_{1x+} - \tilde\lambda_{1x-})$ and $(\tilde\lambda_{2x+} - \tilde\lambda_{2x-})$ in the spin noise

spectrum for a weak magnetic field b_x. A similar perturbative calculation for an in-plane weak magnetic field b_y provides two similar low energy peaks whose positions are sensitive to the imaginary part of the tunneling parameter γ_{nc}.

The positions of frequencies at maxima of these four low energy peaks along with the relative areas of the two peaks at zero magnetic field in Eq. (6) provide a sufficient number of algebraic equations from which all the unknown parameters of the QDM, including relative phases of tunneling rates, can be extracted. The resolution of the split peaks depends on the width of the peaks and the relative separation between them. While the width of the finite-frequency peaks is of the order of 10-50 MHz, the separation between the split peaks depends on the applied magnetic field which can be of the order of 100-1000 Gauss to resolve them.

IV. SPIN NOISE FROM DOUBLE ELECTRON CHARGED QDM

A doubly charged QDM is the smallest testbed where all the steps (initialization, readout, and coherent manipulation of spins) necessary for quantum computation can be realized. In the spin-blockade regime charge transfer between the two dots of the doubly charged QDM can be possible only in the spin-singlet sector of two electrons. This regime has been widely investigated experimentally to probe the electron and nuclear dynamics. Coherent single spin manipulations and gate controllable exchange coupling between spins have been successfully realized in laterally coupled gate-defined QDs[27–29]. Recently coherent optical initialization, control and readout have also been realized by optical means in a vertically stacked QDM[30,31].

For a QDM charged by two electrons there are six spin basis states and four spatial basis states. The spatial parts of the basis states with single electron occupancy in each QD are given by symmetric and antisymmetric wavefunctions $\psi_\pm(\mathbf{r}_1,\mathbf{r}_2) = \frac{1}{\sqrt{2}}(\phi_L(\mathbf{r}_1)\phi_R(\mathbf{r}_2) \pm \phi_R(\mathbf{r}_1)\phi_L(\mathbf{r}_2))$.

The spatial parts of the basis states for the double electron occupancy in the left and the right QD are respectively $\psi_{L,R}(\mathbf{r}_1,\mathbf{r}_2) = \phi_{L,R}(\mathbf{r}_1)\phi_{L,R}(\mathbf{r}_2)$. The six basis spin states are three spin-singlets $|\uparrow\downarrow,0\rangle_s, |0,\uparrow\downarrow\rangle_s, |\uparrow,\downarrow\rangle_s$ and three spin-triplets $|\uparrow,\uparrow\rangle_t, |\downarrow,\downarrow\rangle_t, |\uparrow,\downarrow\rangle_t$. The full antisymmetric two electron basis states are $\psi_L(\mathbf{r}_1,\mathbf{r}_2)|\uparrow\downarrow,0\rangle_s$, $\psi_+(\mathbf{r}_1,\mathbf{r}_2)|\uparrow,\downarrow\rangle_s$, $\psi_R(\mathbf{r}_1,\mathbf{r}_2)|0,\uparrow\downarrow\rangle_s$, $\psi_-(\mathbf{r}_1,\mathbf{r}_2)|\uparrow,\uparrow\rangle_t$, $\psi_-(\mathbf{r}_1,\mathbf{r}_2)|\uparrow,\downarrow\rangle_t$ and $\psi_-(\mathbf{r}_1,\mathbf{r}_2)|\downarrow,\downarrow\rangle_t$. The main difference of the two electron case from the single electron charged QDM is the Coulomb interaction $U(\mathbf{r}_1,\mathbf{r}_2) = e^2/(4\pi\kappa|\mathbf{r}_1-\mathbf{r}_2|)$ between two electrons at position $\mathbf{r}_1,\mathbf{r}_2$, κ is the dielectric constant of the host material. The Coulomb repulsion between two electrons in the left and right dot is given by $V_{LL} = \int d\mathbf{r}_1 \int d\mathbf{r}_2 |\psi_L(\mathbf{r}_1,\mathbf{r}_2)|^2 U(\mathbf{r}_1,\mathbf{r}_2)$ and $V_{RR} = \int d\mathbf{r}_1 \int d\mathbf{r}_2 |\psi_R(\mathbf{r}_1,\mathbf{r}_2)|^2 U(\mathbf{r}_1,\mathbf{r}_2)$. Because the two dots are not identical, the Coulomb energy between two electrons is different in different dots. The Coulomb interaction between electrons for single electron occupancy in each QD is different for spatially symmetric (corresponds to spin-singlet) and antisymmetric (corresponds to spin-triplet) basis states. They are given by $V^s_{LR} = \int d\mathbf{r}_1 \int d\mathbf{r}_2 |\psi_+(\mathbf{r}_1,\mathbf{r}_2)|^2 U(\mathbf{r}_1,\mathbf{r}_2)$ and $V^t_{LR} = \int d\mathbf{r}_1 \int d\mathbf{r}_2 |\psi_-(\mathbf{r}_1,\mathbf{r}_2)|^2 U(\mathbf{r}_1,\mathbf{r}_2)$. Thus for $V_{RR} > 2|\epsilon|$ two electrons mostly stay as one electron in each QD for a lower energy configuration. However as the energy detuning between the two dots increases, i.e., $V_{RR} < 2|\epsilon|$ the ground state becomes $\psi_R(\mathbf{r}_1,\mathbf{r}_2)|0,\uparrow\downarrow\rangle_s$. Therefore by changing the applied electric field we can alter the charge (spatial) configuration of the QDM, which allows us to study the behavior of spin states in the QDM.

Due to the anisotropy in g-factors of electrons in different QDs, the Zeeman energy has two parts, one is the total (absolute value) spin-conserving and the other is the total spin-non-conserving. The Zeeman term in a homogeneous external magnetic field $\mathbf{B}$ is written as $H_Z = \mu_B \mathbf{B}\cdot(\mathbf{g}^e_L\cdot\mathbf{S}_L + \mathbf{g}^e_R\cdot\mathbf{S}_R) = \frac{\mu_B}{2}\mathbf{B}\cdot(\mathbf{g}^e_L+\mathbf{g}^e_R)\cdot(\mathbf{S}_L+\mathbf{S}_R) + \frac{\mu_B}{2}\mathbf{B}\cdot(\mathbf{g}^e_L-\mathbf{g}^e_R)\cdot(\mathbf{S}_L-\mathbf{S}_R)$ where the first term in the second expression conserves the magnitude of total spin $|\mathbf{S}_L+\mathbf{S}_R|$ of the two electrons, and the second term is total spin-non-conserving.

When the applied magnetic field is homogeneous across the QDs, the magnitude of total spin-non-conserving Zeeman term depends on the difference of g-factors. Disregarding the effect of the spin-orbit interactions, the full Hamiltonian of a two-electron charged QDM in the spin basis $\{|\uparrow\downarrow,0\rangle_s, |\uparrow,\downarrow\rangle_s, |0,\uparrow\downarrow\rangle_s, |\uparrow,\uparrow\rangle_t, |\uparrow,\downarrow\rangle_t, |\downarrow,\downarrow\rangle_t\}$ then reads[8,32]

$$H^{(2)} = \begin{pmatrix} V_{LL}+2\epsilon & -\sqrt{2}\gamma_c & 0 & 0 & 0 & 0 \\ -\sqrt{2}\gamma_c & V^s_{LR} & -\sqrt{2}\gamma_c & -\sqrt{2}\delta\eta_- & 2\delta\eta_z & \sqrt{2}\delta\eta_+ \\ 0 & -\sqrt{2}\gamma_c & V_{RR}-2\epsilon & 0 & 0 & 0 \\ 0 & -\sqrt{2}\delta\eta_+ & 0 & V^t_{LR}+2\eta_z & \sqrt{2}\eta_+ & 0 \\ 0 & 2\delta\eta_z & 0 & \sqrt{2}\eta_- & V^t_{LR} & \sqrt{2}\eta_+ \\ 0 & \sqrt{2}\delta\eta_- & 0 & 0 & \sqrt{2}\eta_- & V^t_{LR}-2\eta_z \end{pmatrix}, \tag{8}$$

where $\eta_z = (g_{L\parallel}+g_{R\parallel})b_z/2$, $\eta_\pm \equiv (\eta_x \pm i\eta_y) = (g_{L\perp}+g_{R\perp})(b_x \pm ib_y)/2$ and $\delta\eta_z = (g_{L\parallel}-g_{R\parallel})b_z/2$, $\delta\eta_\pm =$

$(g_{L\perp}-g_{R\perp})(b_x \pm i b_y)/2$. The terms V^s_{LR} and V^t_{LR} account for the Coulomb energy of the singly occupied singlet and triplet spatial states $\psi_\pm(\mathbf{r}_1,\mathbf{r}_2)$[33]. Here we note that the parameters V^s_{LR}, V^t_{LR} and γ_c are not independent in the sense that both γ_c and the difference $V^s_{LR}-V^t_{LR}$ depend on the overlap of the electron wave functions in different QDs. For example, by increasing the tunneling barrier, both of them are expected to be suppressed, so the limit $\gamma_c \to 0$ should be taken with extra care to account for similar changes in $V^s_{LR}-V^t_{LR}$. We have not included γ_{nc} in Eq. (8) as it makes the Hamiltonian much more complex to study analytically, while not making any significant qualitative changes.

Depending on the value of ϵ compared to V_{RR} two electrons can reside in the same dot or in two different dots. In the absence of a magnetic field, the spin-singlet and the spin-triplet sectors are decoupled. Thus the spin-conserving part of the Hamiltonian $H^{(2)}$ reads as

$$H^{(2)}_{sc} = \begin{pmatrix} H_{SS} & 0 \\ 0 & H_{TT} \end{pmatrix}, \tag{9}$$

where the block H_{SS} is a 3×3 matrix in the spin-singlet basis, the block H_{TT} is a 3×3 matrix in the spin-triplet basis, and the off-diagonal blocks connecting the two spin sectors are zero in the absence of spin-non-conserving interactions.

There is no mixing between basis states in the triplet sectors. In typical QDMs, $V_{LL}, V_{RR} \approx 1$ meV and depend on the dielectric constant κ of the host material. The spin-conserving tunneling γ_c and the Coulomb interaction strengths V^s_{LR}, V^t_{LR} between electrons/holes in different dots depend on the distance between the dots and the height of the barrier between them. The accessibility of the spin noise spectroscopy technique in experiments has been limited to GHz (order of μeV) frequency scale so here we mostly concentrate on the regime of a characteristic tunneling frequency below 1 GHz. Recently, ultrafast SNS was introduced that extended the range of applications to systems with a much faster dynamics, up to hundreds of GHz[34,35]. Our results, however, can be easily extended to other frequency regimes.

There can be two types of low frequency/energy resonances in the doubly charged QDMs. A single finite-frequency peak in the spin noise spectrum develops when the QDs are almost degenerate in energy, i.e., $\epsilon \approx 0$. It arises via the virtual transition of electron between the singlet $|\uparrow,\downarrow\rangle_s$ of single electrons in each QD and the singlets $|\uparrow\downarrow,0\rangle_s$, $|0,\uparrow\downarrow\rangle_s$ of two electrons in the same left or right QD, leading to the effective exchange coupling between spins. Figure 2(a) shows that the spin noise spectrum at $\epsilon \approx 0$ for $V_{LL} \approx V_{RR} \gg \gamma_c, V^s_{LR}, V^t_{LR}$ has one zero frequency peak and one finite frequency peak at $[(V^s_{LR}-V^t_{LR}) - 2\gamma_c^2/V_{RR} - 2\gamma_c^2/V_{LL}]/h$ (in the leading order of γ_c^2/V_{RR} and γ_c^2/V_{LL}). If the bias ϵ is set exactly

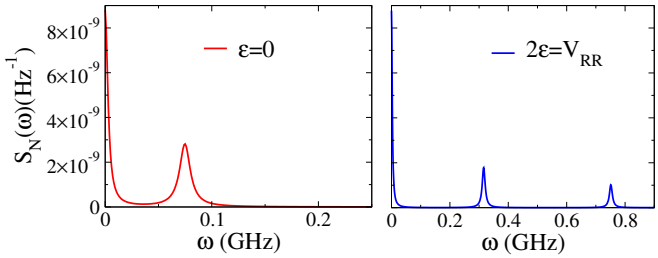

FIG. 2. Low-frequency spin noise power spectrum for a double electron charged QDM. The parameters are $V_{RR} = V_{LL} =$ 1meV, $\gamma_c = V^t_{LR} = 1.5\mu$eV, $V^s_{LR} = 1.2\mu$eV. Broadening width of the zero frequency and finite frequency peaks are respectively 0.025μeV and 0.05μeV. The ratio of coupling $\alpha/\beta = 9$.

at resonance, the spin noise correlator reads

$$\langle S^T_z(t) S^T_z(0)\rangle = \frac{(\alpha+\beta)^2}{12} + \frac{(\alpha-\beta)^2}{12} \times \cos\left(V^s_{LR} - V^t_{LR} - \frac{2\gamma_c^2}{V_{RR}} - \frac{2\gamma_c^2}{V_{LL}}\right) t. \tag{10}$$

The ability to observe (or resolve) the finite frequency peak depends on its width, which is determined mostly by the decoherence rate. The width of the zero frequency peak is controlled by the spin relaxation time, which is of the order of 1 MHz [24] (see Fig. 2), i.e., it is much narrower than the width of the finite-frequency peak. Two non-zero low frequency peaks can occur in the spin noise spectrum when the bias $2\epsilon \approx V_{RR}$. Then the singlet state $|0,\uparrow\downarrow\rangle_s$ of two electrons in the right QD becomes degenerate with the singlet $|\uparrow,\downarrow\rangle_s$ and triplet $|\uparrow,\downarrow\rangle_t$ states of single electrons in each QD with total $S_z = 0$. In typical QDMs the mixing by spin-conserving tunneling of one out of three singlet basis states is quite suppressed at a finite ϵ because $V_{LL} \approx V_{RR} \gg \gamma_c, V^s_{LR}, V^t_{LR}$. For $\epsilon > 0$ the singlet basis state $|\uparrow\downarrow,0\rangle_s$ with energy $V_{LL}+2\epsilon$ is far detuned from the other two singlet basis states $|\uparrow,\downarrow\rangle_s$, $|0,\uparrow\downarrow\rangle_s$, and we calculate mixing of the last two basis states. The hybridized states of the two singlet states are $|S_-\rangle = \cos\theta|\uparrow,\downarrow\rangle_s + \sin\theta|0,\uparrow\downarrow\rangle_s$ and $|S_+\rangle = \sin\theta|\uparrow,\downarrow\rangle_s - \cos\theta|0,\uparrow\downarrow\rangle_s$ with energy eigenvalues

$$E_{S\mp} = \frac{V^s_{LR}+V_{RR}-2\epsilon}{2} \mp \sqrt{\frac{(V_{RR}-V^s_{LR}-2\epsilon)^2}{4} + 2\gamma_c^2}, \tag{11}$$

and θ is the mixing angle between $|\uparrow,\downarrow\rangle_s$ and $|0,\uparrow\downarrow\rangle_s$. When the bias $2\epsilon \approx V_{RR}$ the effective Hamiltonian in the basis states of $|S_-\rangle$, $|S_+\rangle$ and $|\uparrow,\downarrow\rangle_t$ states is a diagonal 3×3 matrix with entries, $E_{s-}|_{2\epsilon\approx V_{RR}} \equiv \lambda_- = \frac{V^s_{LR}}{2} - \sqrt{\frac{{V^s_{LR}}^2}{4} + 2\gamma_c^2}$, $E_{s+}|_{2\epsilon\approx V_{RR}} \equiv \lambda_+ = \frac{V^s_{LR}}{2} + \sqrt{\frac{{V^s_{LR}}^2}{4} + 2\gamma_c^2}$ and V^t_{LR} respectively. The spin noise correlators at $2\epsilon \approx$

V_{RR} are given by

$$\langle S_z^T(t)S_z^T(0)\rangle = \frac{(\alpha+\beta)^2}{12} + \frac{(\alpha-\beta)^2}{12}\big(\sin^2\phi \times \cos(\lambda_+ - V_{LR}^t)t + \cos^2\phi\cos(\lambda_- - V_{LR}^t)t\big), \quad (12)$$

$$\sin\phi = \frac{-\sqrt{2}\gamma_c}{\sqrt{(V_{LR}^s-\lambda_+)^2+2\gamma_c^2}},$$

$$\cos\phi = \frac{(V_{LR}^s-\lambda_+)}{\sqrt{(V_{LR}^s-\lambda_+)^2+2\gamma_c^2}}, \quad (13)$$

where $\phi = \theta|_{2\epsilon\approx V_{RR}}$. From the relative area of the zero-frequency and finite-frequency peaks in Eq. (10) we determine the ratio α/β. Similarly the relative area of the two finite-frequency peaks in Eq. (12) can be measured with a good precision, and the ratio is given by $2\gamma_c^2/\lambda_-^2$. The measured central frequency of the finite-frequency peak in Eq. (10) and the two finite-frequency peaks in Eq. (12), and the relative area ($\tan^2\phi$) of the two finite-frequency peaks in Eq. (12) provide us four relations for the four unknown parameters $\gamma_c, V_{LR}^s, V_{LR}^t, V_{RR}$ of the QDM. These relations can be solved to find the four unknown parameters. Similarly, by tuning negative 2ϵ near V_{LL} we will have spin noise correlators as in Eq. (12) with V_{RR} replaced by V_{LL}.

Finally we discuss how the low-frequency spin noise spectrum would modify in the presence of a homogeneous total spin-conserving magnetic field, i.e., $\eta_z, \eta_\pm \neq 0$ and $\delta\eta_z, \delta\eta_\pm = 0$. We can have $\eta_z, \eta_\pm \neq 0$ and $\delta\eta_z, \delta\eta_\pm = 0$ when $\mathbf{g}_L^e = \mathbf{g}_R^e$ or $\mathbf{S}_L = \mathbf{S}_R$. However, we here discuss the spin noise spectrum in a homogeneous magnetic field for same g-factors of the left and right dot electrons, i.e., $\mathbf{g}_L^e = \mathbf{g}_R^e$. In the presence of $\eta_z, \eta_\pm \neq 0$ at a bias $\epsilon \approx 0$, the finite-frequency peak additionally splits into three peaks with mean frequencies of two of them shifted by $\pm 2\bar{\eta}$ from the original positions, where the applied scaled magnetic field $\bar{\eta} = \sqrt{\eta_x^2+\eta_y^2+\eta_z^2}$. The peak that was initially centered at the zero frequency splits into a zero-frequency peak and a finite-frequency peak at a characteristic Larmor frequency $2\bar{\eta}$. Thus there will be totally four finite-frequency peaks and a zero frequency peak at a bias $\epsilon \approx 0$. Similarly we have total seven finite-frequency peaks and one zero-frequency peak at a bias $2\epsilon \approx V_{RR}$ in the presence of a homogeneous applied magnetic field.

Here we have not considered the effect of spin-non-conserving interactions such as the spin-orbit coupling on the spin-noise spectrum of the doubly charged QDM[7]. The eigenvalues of the Hamiltonian of the doubly charged QDM in the presence of spin-orbit coupling would remain doubly degenerate as long as time-reversal symmetry is preserved. The spin noise spectrum in the presence of spin-orbit coupling would consequently be similar to the spectrum which we have derived in the absence of spin-orbit coupling. However the central frequency of the finite-frequency peaks and the relative area of the peaks would be renormalized.

V. CONCLUSION

We discussed the possibility of characterization of quantum dot molecules by the spin noise spectroscopy. We showed that this approach reveals valuable information about parameters of the QDMs, including coherent tunneling between QDs, without perturbing the system from the equilibrium.

One of our goals was to emphasize the fact that spin-noise spectroscopy, when applied to complex nanostructures, is not restricted to measurements of a total spin dynamics. We predict that the Faraday effect should be strongly sensitive not only to magnitude but also to the positions of the spins. This allows one to resolve coherent tunneling as well as exchange-type spin-spin interactions even if the total spin is conserved in a process. For example, the appearance of all finite frequency peaks discussed in Sec. IV at zero magnetic field would be impossible without the difference between coupling parameters α and β. Observations of such peaks may become an alternative approach to study coherent tunneling in complex nanostructures.

We explored the spin noise power spectrum of single and double electron charged QDM in the presence of an applied electric and/or magnetic field. We argued, in particular, that the relative area of the noise power peaks contains valuable information for the characterization of the QDMs. For a single charged QDM, we derived an explicit expression for the spin noise power in a most general type of Hamiltonian allowed by the time-reversal symmetry. Both spin conserving and spin non-conserving tunneling amplitudes (as well as their relative phase) can be obtained by studying the response of the noise power spectrum to a weak in-plane magnetic field. A doubly charged QDM can be explored by similar means. Away from specific resonances, the spin noise power at finite frequencies will be suppressed. When the bias electric field is tuned to specific resonances, the tunneling of electrons/holes between quantum dots leads to the appearance of new high frequency peaks, whose area and position can be used to obtain the effective tunneling rate and other coupling parameters.

We expect that measurements of the noise power spectrum should have particular advantages over other approaches such as laser absorption and spin-echo experiments, when characterization of spin coherence is needed at frequencies below 1 GHz, e.g. the photoluminescence approach is usually resolution limited to several GHz. We believe our work will provide a useful guidance for experimental characterization of quantum nanostructures, in particular QDMs, by means of spin noise spectroscopy.

Finally we note that spin noise spectroscopy of a single hole spin localized in an (InGa)As quantum dot has been demonstrated in a recent experiment[36].

VI. ACKNOWLEDGMENTS

We thank D. L. Smith and S. A. Crooker for useful discussions. Work at LANL was carried out under the auspices of the Project No. LDRD/20110189ER and the National Nuclear Security Administration of the U.S. Department of Energy at Los Alamos National Laboratory under Contract No. DE-AC52-06NA25396.

[1] D. Loss and D. P. DiVincenzo, Phys. Rev. A **57**, 120 (1998).

[2] F. H. L. Koppens, K.C. Nowack, and L.M.K. Vandersypen, Phys. Rev. Lett. **100**, 236802 (2008).

[3] M. Bayer, P. Hawrylak, K. Hinzer, S. Fafard, M. Korkusinski, Z. R. Wasilewski, O. Stern, and A. Forchel, Science **291**, 451 (2001).

[4] H. J. Krenner, M. Sabathil, E. C. Clark, A. Kress, D. Schuh, M. Bichler, G. Abstreiter, and J. J. Finley, Phys. Rev. Lett. **94**, 057402 (2005).

[5] E. A. Stinaff, M. Scheibner, A. S. Bracker, I. V. Ponomarev, V. L. Korenev, M. E. Ware, M. F. Doty, T. L. Reinecke, and D. Gammon, Science **311**, 636 (2006).

[6] D. D. Awschalom, D. Loss, and N. Samarth, *Semiconductor Spintronics and Quantum Computation* (Springer, New York, 2002).

[7] A. Greilich, Ş. C. Bădescu, D. Kim, A. S. Bracker, and D. Gammon, Phys. Rev. Lett. **110**, 117402 (2013).

[8] M. F. Doty, M. Scheibner, A. S. Bracker, I. V. Ponomarev, T. L. Reinecke, and D. Gammon, Phys. Rev. B **78**, 115316 (2008).

[9] M. Scheibner, M. F. Doty, I. V. Ponomarev, A. S. Bracker, E. A. Stinaff, V. L. Korenev, T. L. Reinecke, and D. Gammon, Phys. Rev. B **75**, 245318 (2007).

[10] L. Robledo, J. Elzerman, G. Jundt, M. Atatüre, A. Högele, S. Fält, and A Imamoglu, Science **320**, 772 (2008).

[11] S. A. Crooker, J. Brandt, C. Sandfort, A. Greilich, D. R. Yakovlev, D. Reuter, A. D. Wieck, and M. Bayer, Phys. Rev. Lett.**104**, 036601 (2010).

[12] Y. Li, N. Sinitsyn, D. L. Smith, D. Reuter, A. D. Wieck, D. R. Yakovlev, M. Bayer, and S. A. Crooker, Phys. Rev. Lett. **108**, 186603 (2012).

[13] M. Atature, J. Dreiser, A. Badolato, and A. Imamoglu, Nature Phys. **3**, 101 (2007).

[14] A. V. Kuhlmann, J. Houel, A. Ludwig, L. Greuter, D. Reuter, A. D. Wieck, M. Poggio, and R. J. Warburton, arXiv:1301.6381v1 (2013).

[15] S. A. Crooker, D. G. Rickel, A. V. Balatsky, and D. L. Smith, Nature (London) **431**, 49 (2004).

[16] E. B. Aleksandrov and V. S. Zapasskii, Zh. Eksp. Teor. Fiz. **81**, 132 (1981) [JETP **54**, 64 (1981)].

[17] M. Oestreich, M. Römer, R. J. Haug, and D. Hägele, Phys. Rev. Lett. **95**, 216603 (2005).

[18] S. A. Crooker, L. Cheng, and D. L. Smith, Phys. Rev. B **79**, 035208 (2009).

[19] G. M. Müller, M. Römer, D. Schuh, W. Wegscheider, J. Hübner, and M. Oestreich, Phys. Rev. Lett. **101**, 206601 (2008).

[20] G. M. Müller, M. Oestreich, M. Römer, and J. Hübner, Physica E **43**, 569 (2010).

[21] Y. V. Pershin, V. A. Slipko, D. Roy, and N. A. Sinitsyn, App. Phys. Lett. **102**, 202405 (2013).

[22] B. Mihaila, S. A. Crooker, D. G. Rickel, K. B. Blagoev, P. B. Littlewood, and D. L. Smith, Phys. Rev. A **74**, 043819 (2006).

[23] V. S. Zapasskii, A. Greilich, S. A. Crooker, Yan Li, G. G. Kozlov, D. R. Yakovlev, D. Reuter, A. D. Wieck, and M. Bayer, Phys. Rev. Lett. **110**, 176601 (2013).

[24] N. A. Sinitsyn, Y. Li, S. A. Crooker, A. Saxena, and D. L. Smith, Phys. Rev. Lett. **109**, 166605 (2012).

[25] A. S. Bracker, M. Scheibner, M. F. Doty, E. A. Stinaff, I. V. Ponomarev, J. C. Kim, L. J. Whitman, T. L. Reinecke, and D. Gammon, App. Phys. Lett. **89**, 233110 (2006).

[26] B. Eble, C. Testelin, P. Desfonds, F. Bernardot, A. Balocchi, T. Amand, A. Miard, A. Lemaître, X. Marie, and M. Chamarro, Phys. Rev. Lett. **102**, 146601 (2009)

[27] J. R. Petta, A. C. Johnson, J. M. Taylor, E. A. Laird, A. Yacoby, M. D. Lukin, C. M. Marcus, M. P. Hanson, and A. C. Gossard, Science **309**, 2180 (2005).

[28] F. H. L. Koppens, C. Buizert, K. J. Tielrooij, I. T. Vink, K. C. Nowack, T. Meunier, L. P. Kouwenhoven, and L. M. K. Vandersypen, Nature (London) **442**, 766 (2006).

[29] K. C. Nowack, F. H. L. Koppens, Y. V. Nazarov, and L. M. K. Vandersypen, Science **318**, 1430 (2007).

[30] D. Kim, S. G. Carter, A. Greilich, A. S. Bracker, and D. Gammon, Nature Physics **7**, 223 (2011).

[31] A. Greilich, S. G. Carter, D. Kim, A. S. Bracker, and D. Gammon, Nat. Photonics **5**, 702 (2011).

[32] D. Stepanenko, M. Rudner, B. I. Halperin, and D. Loss, Phys. Rev. B **85**, 075416 (2012).

[33] G. Burkard, D. Loss, and D. P. DiVincenzo, Phys. Rev. B, **59**, 2070 (1999).

[34] F. Berski, H. Kuhn, J. G. Lonnemann, J. Hübner, and M. Oestreich, Preprint arXiv:1207.0081 (2012).

[35] J. Hübner, J. G. Lonnemann, P. Zell, H. Kuhn, F. Berski, and M. Oestreich, Opt. Express **21**, 5872 (2013).

[36] R. Dahbashi, J. Hübner, F. Berski, K. Pierz, and M. Oestreich, arXiv:1306.3183 (2013).